



저작자표시-비영리-변경금지 2.0 대한민국

이용자는 아래의 조건을 따르는 경우에 한하여 자유롭게

- 이 저작물을 복제, 배포, 전송, 전시, 공연 및 방송할 수 있습니다.

다음과 같은 조건을 따라야 합니다:



저작자표시. 귀하는 원저작자를 표시하여야 합니다.



비영리. 귀하는 이 저작물을 영리 목적으로 이용할 수 없습니다.



변경금지. 귀하는 이 저작물을 개작, 변형 또는 가공할 수 없습니다.

- 귀하는, 이 저작물의 재이용이나 배포의 경우, 이 저작물에 적용된 이용허락조건을 명확하게 나타내어야 합니다.
- 저작권자로부터 별도의 허가를 받으면 이러한 조건들은 적용되지 않습니다.

저작권법에 따른 이용자의 권리는 위의 내용에 의하여 영향을 받지 않습니다.

이것은 [이용허락규약\(Legal Code\)](#)을 이해하기 쉽게 요약한 것입니다.

[Disclaimer](#)

공학석사 학위논문

**Shape Memory Polyurethane Foam for
Thermal Insulation**

단열 성능 향상을 위한
형상기억 발포폴리우레탄에 관한 연구

2014년 2월

서울대학교 대학원

재료공학부

김 지 선

Shape Memory Polyurethane Foam for Thermal Insulation

단열 성능 향상을 위한
형상기억 발포폴리우레탄에 관한 연구

지도 교수 윤 재 룬

이 논문을 공학석사 학위논문으로 제출함
2014 년 2월

서울대학교 대학원
재료공학부
김 지 선

김지선의 석사 학위논문을 인준함
2014년 2월

위 원 장 _____ 강 태 진 (인)

부위원장 _____ 윤 재 룬 (인)

위 원 _____ 유 응 렬 (인)

**Shape Memory Polyurethane Foam for
Thermal Insulation**

Advisor: Jae Ryoun Youn

by
Ji Sun Kim

2014

Department of Materials Science and Engineering

Graduate School

Seoul National University

ABSTRACT

Foam materials are widely used as insulators, because they have a structure stability as well as a low thermal conductivity. In order to manufacture an efficient insulation material, shape memory polyurethane (SMPU) foam was prepared and its thermal conductivity was measured. The relation between thermal conductivity and microstructure of the foam was studied. The experimental thermal conductivities of the SMPU foam specimens were compared to theoretical thermal conductivities of those.

SMPU was synthesized by using prepolymerization method. Differential Scanning Calorimeter (DSC) was used to examine the transition temperature (T_{tr}) of SMPU. SMPU foams were obtained by the salt leaching method and prepared with respect to particle size of salts in order to control the pore size of the SMPU foam. Hybrid foam was fabricated by mixing two different sizes of NaCl particles and functionally gradient foam was also manufactured by laminating layers of three different sizes of NaCl particles. The thermal conductivity, mechanical property, shape memory properties were characterized and thermal resistance of various specimens were also calculated to investigate adiabatic properties.

SMPU foam has advantages of space occupancy and wearability because it can be fixed to thin shape at room temperature. When SMPU foam recovers to its original thickness at above T_{tr} , the thermal resistance is

increased. SMPU foam is expected to be used in insulation field as an intelligent adiabatic material.

Keywords: shape memory polyurethane, foam material, thermal conductivity, insulation material

Student number: 2012-20588

CONTENTS

ABSTRACT

LIST OF FIGURES AND TABLES

I. INTRODUCTION	1
1.1. Polyurethane foam	1
1.2. Shape memory polyurethane	2
1.2.1. Advantage of Shape Memory Polymer (SMP)	2
1.2.2. Structure and mechanism of SMPU	3
1.3. Heat transfer in foam material	5
1.4. Objective of this study	6
II. EXPERIMENTS	8
2.1. Materials	8
2.2. Preparation of the specimen	8
2.2.1. Synthesis of SMPU	8
2.2.2. SMPU film	11
2.2.3. SMPU foam	11
2.3. Measurements and characterization	14
2.3.1. Differential Scanning Calorimeter (DSC)	14
2.3.2. Particle Size Analysis	14

2.3.3. Morphological Analysis	14
2.3.4. Porosity	15
2.3.5. Thermal Conductivity Measurements	15
2.3.6. Shape memory effect	15
2.3.7. Mechanical property	18
III. RESULTS AND DISCUSSION	19
3.1. Morphological properties	19
3.1.1. Particle sizes of NaCl	19
3.1.2. SEM images of SMPU foam	24
3.1.3. Porosity of SMPU foam	30
3.2. Thermal properties	34
3.2.1. DSC results	34
3.2.2. Thermal conductivity	36
3.2.3. Thermal resistance	40
3.3. Shape memory effect of SMPU foam	43
3.3.1. Shape recovery and fixity	43
3.3.2. Shape memory repeatability	46
3.4. Mechanical properties	48
3.5. Analytic modeling	50
3.5.1. Heat transfer theory of SMPU foam	50
3.5.2. Prediction of thermal conductivity of SMPU foam	53

V. CONCLUSION 56

REFERENCES

KOREAN ABSTRACT

LIST OF FIGURES AND TABLES

Figure 1.1. Molecular mechanism of the thermally induced shape memory polymer with $T_{tr} = T_m$ of soft segment.

Figure 2.1. Fabrication process of the shape memory polyurethane by using prepolymerization method.

Figure 2.2. Chemical structure of 4, 4'-diphenylmethane diisocyanate (MDI), 1, 4-Butanediol (BD), Poly caprolactone diol (PCL diol).

Figure 2.3. Manufacture process of SMPU foam by using salt leaching method.

Figure 2.4. Experimental procedure of shape memory effect measurement for SMPU foam.

Figure 3.1. SEM images of various size NaCl particles filtered by using different sieves. Average particle sizes of the NaCl were (a) 413.8 (b) 242 (c) 127.5 μm

Figure 3.2. Size distribution of the filtered NaCl particles. Average particle sizes of the NaCl were (a) 413.8 (b) 242 (c) 127.5 μm

Figure 3.3. SEM images of cross sectional images of SMPU foams: (a) SMPU foam-400 (b) SMPU foam-200 (c) SMPU foam-100 (d) Hybrid foam (e) Functionally gradient foam (f) Functionally gradient foam

Figure 3.4. SEM images of cross sectional images of SMPU foam-400: (a) original shape (b) compressed shape (c) recovered shape

Figure 3.5. Porosity of different SMPU foams having different size of pore (SMPU foam-400, SMPU foam-200, SMPU foam-100) and different structure (hybrid foam, functionally gradient foam).

Figure 3.6. Porosity of SMPU foam-400 with the change of the specimen (original shape, compressed shape, recovered shape).

Figure 3.7. The DSC result of the synthesized SMPU which was measured at a heating rate of 10 °C/min.

Figure 3.8. Thermal conductivity of the synthesized SMPU and SMPU foams.

Figure 3.9. Thermal conductivity of the SMPU foams having different pores sizes (SMPU foam-400, SMPU foam-200, SMPU foam-100) and different structure (hybrid foam, functionally gradient foam).

Figure 3.10. Thermal conductivity of SMPU foam with change of thickness of specimen.

Figure 3.11. Thermal resistance of SMPU foam with change of thickness of specimen.

Figure 3.12. Shape recovery of SMPU foam specimens.

Figure 3.13. Shape fixity of SMPU foam specimens.

Figure 3.14. The compressive stress-strain curves for the shape memory repeatability of the SMPU foam at a compressive strain rate of 10 mm/min.

Figure 3.15. The compressive stress-strain curves of the SMPU foam at a compressive strain rate of 10 mm/min.

Figure 3.16. Radiation conductivity vs. pore size when density is fixed.

Figure 3.17. Thermal conductivity measured and predicted for different SMPU foam specimens.

Table 2.1. NaCl particle size and structures aimed at manufacturing various samples.

Table 3.1. Porosity of SMPU foam specimens.

Table 3.2. Porosity changes with the shape of SMPU foam (original shape, compressed shape, recovered shape).

Table 3.3. Thermal conductivity of SMPU foam specimens.

Table 3.4. Thermal resistance of SMPU foam with change of thickness.

Table 3.5. Shape recovery and fixity of SMPU foams.

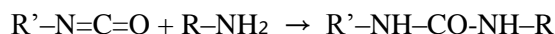
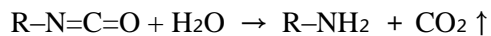
Table 3.6. Shape recovery and fixity of SMPU foams with increasing of number of cycles.

I. INTRODUCTION

1.1. Polyurethane foam

Polyurethane (PU) is a polymer composed of urethane links and is formed by reacting diisocyanates with polyols. PU is a polymer having a wide scope of mechanical and chemical properties. Therefore, it is used in a broad range of industrial applications such as insulation material, furniture, packaging and appliances. As occasion demands, PU can be produced to various forms such as coatings, adhesives, fibers, thermoplastic elastomers and foams.

In general, PU foams were used as insulating materials because they have a low thermal conductivity in addition to a structural stability. There are several methods to produce PU foam such as chemical blowing agent method, physical blowing method and salt leaching method. The distilled water is typically used as chemical blowing agent. It reacts with isocyanate to generate carbon dioxide and amine which will react with isocyanate to form polyurea as following equation.



Foam structure is formed when the carbon dioxide occurred in the mixture.

Additional Isocyanate is needed to react with water [1]. Chlorofluorocarbons (CFC) and hydrochlorofluorocarbon (HCFC) gases are widely used as physical blowing agent. As CFC or HCFC gases change phases from liquid to vapor, a cellular structure is formed [2-4].

In this study, PU foams were manufactured by the salt leaching method. The salt leaching method is one of particulate leaching method. Porous materials are prepared by the salt leaching method as following steps. First, polymer dissolves in solvent and then salt particles were mixed evenly in the solution. The solvent is volatilized completely from composite. After removing the solvent from the composite, the salt particles leach from the composite by immersing the composite in water. This method is widely utilized in biomaterial for medical application[5]. It has several advantages. The manufacturing process is simple and it is easy to control the porosity and the pore size of the foam by changing the size and the amount of the salt particles [6].

1.2. Shape memory polyurethane

1.2.1. Advantage of Shape Memory Polymer (SMP)

Polyurethane is one of the Shape Memory Polymer (SMP) which can move actively in response to an external stimulus such as heat, light,

moisture, pH and electric field [7]. Recent research on SMP is attracting attention and widely studied. Features of SMP are more useful, particularly compared with Shape Memory Alloy (SMA). A process to manufacture SMP is easier and simpler than SMA. SMP has a large range of structure deformation and the price of SMP is cheaper than that of SMA. Properties of SMP can be easily changed by blending filler. It is nontoxic material and can be utilized as a biodegradable polymer and biocompatible devices to interface with human bodies. SMP is light and can be produced in the foam structure readily. Therefore it has a wide range of applications in aerospace devices [8, 9].

1.2.2. Structure and mechanism of SMPU

Shape memory effect has been observed with various polymers such as polynorbornene, styrene-butadiene copolymer and polyurethane [10, 11]. Polyurethane has been commonly used as Shape Memory Polymer. Fig. 1.1 shows the mechanism of the shape memory effect of SMP based on the formation of phase separated structure.

Shape memory polyurethane (SMPU) is a block copolymer which consists of hard segments and soft segments. These two segments have phase separated structure because of thermodynamic incompatibility. Physical properties of SMPU are influenced by the degree and structure of

the phase separation. Therefore, SMPU with varied properties can be manufactured by controlling the ratio of the hard segment and soft segment and adjusting molecular weights of each segment [9].

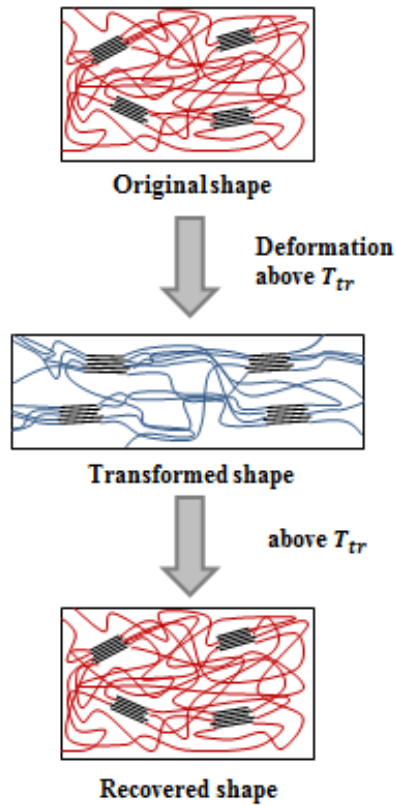


Figure 1.1. Molecular mechanism of the thermally induced shape memory polymer with $T_{tr} = T_m$ of soft segment.

1.3. Heat transfer in foam material

A polymer foam consists of many pores and solid walls. Therefore thermal conductivity of a polymer foam is composed with combinations of conduction, convection, and radiation. First, conduction heat transfer must be considered. Conduction heat transfer through the solid and the gas in the pore is the most important contribution to the thermal conductivity of the foam. Convection heat transfer by the gas in the cells can be ignored when the cell diameter is smaller than 1.5 mm [12]. The space of each cell in the general polymer foams is small enough to neglect the effect of the convection heat transfer.

The contribution of the radiation heat transfer in the polymer foams is smaller than the conduction through the solid walls and the gas in the pore. In the earlier studies, heat transfer caused by radiation was ignored, however the contribution of the radiation cannot be neglected when the cell size is large or at the high temperature. If the pore size of the polymer foams is larger than 200 μm , the contribution of the radiation heat transfer is more than 20%. However, the contribution of the radiation can be ignored when the cell size of the foam is smaller than 10 μm .

There are two methods in order to integrate the heat transfer through various paths in the polymer foam. First method is theoretically coupling each contribution and second method is simply adding each

contribution to the overall heat transfer. The latter method is widely used because of its simplification as well as small error range. Therefore, the overall thermal conductivity of a polymer foam can be expressed by the equation (1) [13].

$$\lambda_{foam} = [\lambda^{gas} + \lambda^{solid}]_{conduction} + \lambda_{radiation} \quad (1)$$

where λ_{foam} denotes the overall thermal conductivity, $[\lambda^{gas} + \lambda^{solid}]_{conduction}$ is the conductivity arise from the conduction through the gas and solid, and $\lambda_{radiation}$ is the conductivity caused by the radiation in the cells [3, 14].

1.4. Objective of this study

In this study, SMPU was synthesized to prepare the SMPU foam as an insulating material. The SMPU foam was manufactured by the salt leaching method. The size of salt particles was controlled in order to prepare foams having different pore size respectively. Thermal and mechanical properties of the SMPU foam were characterized to analyze the property transformation by changing the pore size of the SMPU foam. Moreover, the thermal conductivity of SMPU foam specimens were measured at different form such as original shape, compressed shape and recovered shape. In addition, shape memory properties of the SMPU foam were also investigated by changing the ambient temperature to verify the shape memory effect.

Theoretical equations of the heat transfer in foam materials were also reported in this study. Thermal conductivities varied with the pore size were predicted and compared with experimental values.

II. EXPERIMENTS

2.1. Materials

Poly caprolactone diol (PCL diol, $M_n=4,000$ g/mol, Perstop, UK), 4, 4'-diphenylmethane diisocyanate (MDI, Junsei Chemical, Japan), 1, 4-Butanediol (BD, Sigma Aldrich, USA) were prepared to synthesize SMPU. Chemical structures of PCL diol, MDI and BD were shown in Fig. 2.2.

In order to manufacture SMPU foam, Tetrahydrofuran (THF, Daejung Chemicals, Korea) and sodium chloride (NaCl, Daejung Chemicals, Korea) were prepared. THF was used as solvent for manufacturing SMPU solution and NaCl particles were utilized to create pores of SMPU foam by dissolving in water. Pestle and mortar, micro size sieves were utilized to control the size of NaCl particles.

2.2. Preparation of the specimen

2.2.1. Synthesis of SMPU

The molar ratio for SMPU synthesis was 6 : 1 : 5 for MDI : PCL diol : BD as optimum mixture condition. As shown in Fig. 2.1, SMPU were synthesized with prepolymerization method. MDI and PCL diol were mixed

to prepare prepolymer. MDI was used to compose the hard segment and PCL diol was made up soft segment. BD which was used as a chain extender was added to prepolymer for increasing the degree of polymerization. After mixing, SMPU was dried at room temperature.

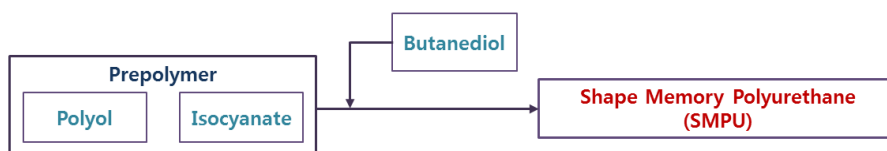


Figure 2.1. Fabrication process of the shape memory polyurethane by using prepolymerization method.

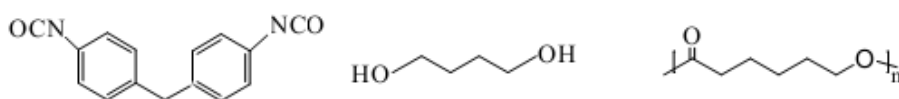


Figure 2.2. Chemical structure of 4, 4'-diphenylmethane diisocyanate (MDI), 1, 4-Butanediol (BD), Poly caprolactone diol (PCL diol)

2.2.2. SMPU film

As a reference specimen, SMPU film was prepared. SMPU pellets were melted down and compressed by using hot press. The specimen was prepared with a size of 20 mm (length) x 20 mm (width) x 3 mm (thickness).

2.2.3. SMPU foam

SMPU pellets were dissolved in THF which was used as solvent to manufacture the SMPU foam. The concentration of SMPU in the solution was 25 wt. %. The NaCl particles were grinded and filtered by several sieves with micro sizes of mesh. The SMPU solution and the filtered NaCl particles were well mixed, the volume ratio was 10 : 8 for SMPU solution : NaCl. The mixed solution was dried in 40°C for 2~3 days until THF was volatilized completely. In order to leach the NaCl from the SMPU/NaCl composite, the specimen was immersed in water. After leaching the NaCl thoroughly, the specimen was dried at room temperature. Fig. 2.3 shows the overall process to manufacture SMPU foam [15, 16]. Various specimens manufactured and analyzed in this study are listed in Table 2.1.

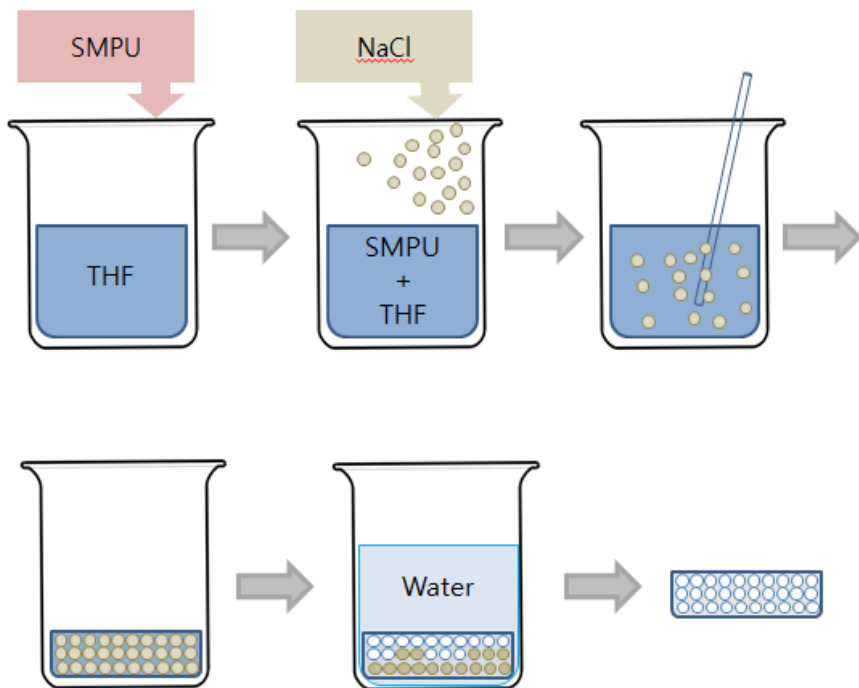
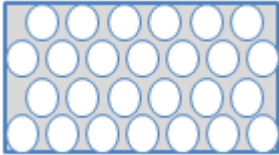
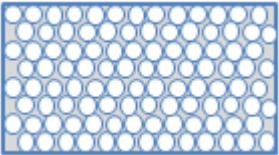
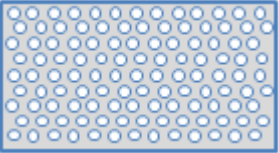
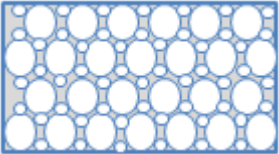
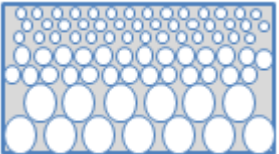


Figure 2.3. Manufacture process of SMPU foam by using salt leaching method.

Table 2.1. NaCl particle size and structures aimed at manufacturing various samples.

Samples	Used NaCl particle size	Structure
SMPU foam-400	400 μm	uniform structure 
SMPU foam-200	200 μm	uniform structure 
SMPU foam-100	100 μm	uniform structure 
Hybrid foam	400 and 100 μm	mixed structure having pores of two different sizes 
Functionally gradient foam	400, 200 and 100 μm	laminated structure 

2.3. Measurements and characterization

2.3.1. Differential Scanning Calorimeter (DSC)

The transition temperature (T_{tr}) of SMPU was measured with Differential Scanning Calorimeter (DSC 200 F3 Maia, Netzsch Korea) from -20°C to 250°C at a heating rate of $10^{\circ}\text{C}/\text{min}$.

2.3.2. Particle Size Analysis

In order to measure the average diameter of NaCl particles, the size controlled NaCl samples were prepared by grinding and filtering with sieves. Isopropyl alcohol (IPA) was used as dispersion solution. A particle size analyzer (Microtrac Inc., S3500 Series) based on the laser light diffraction method was used in order to determine the particle size distribution of the samples.

2.3.3. Morphological Analysis

The cell morphology of the size controlled NaCl particles and the cross section of SMPU foam were observed with a Field-Emission Scanning Electron Microscope (FE-SEM, JSM-7600F).

2.3.4. Porosity

In general, the porosity of the foam material can be calculated from the change of the density.

$$V_g = \left(1 - \frac{\rho_f}{\rho_p}\right) \times 100 \quad (2)$$

where ρ_p denotes the density of the polymer forming foam material and ρ_f is the density of the foam material [17-19].

2.3.5. Thermal Conductivity Measurements

Thermal conductivity analyzer (TCi, C-THERM) was employed to measure the thermal conductivity of the specimen. To measure the thermal conductivity, the SMPU foam specimens were prepared with a size of 20 mm (length) \times 20 mm (width) \times 10mm (thickness). Modified transient plane source (MTPS) method was used. Thermal conductivity analyzer has a sensor which has a central heater/sensor element surrounded by a guard ring which generates heat. The one-sided interfacial reflectance sensor supply heat to the sample.

2.3.6. Shape memory effect

Shape memory effects were measured with a temperature controlled Universal Testing Machine (UTM) (WL2100, WITHLAB, Korea). Fig. 2.4 shows experimental procedure of the shape memory effect measurement for SMPU foam. The SMPU foam was cut into dimensions of 35 mm (diameter) x 20 mm (thickness). The specimen was heated to $T_{tr} + 20^{\circ}\text{C}$, and then it was compressed to 80% at $T_{tr} + 20^{\circ}\text{C}$ and cooled down to $T_{tr} - 20^{\circ}\text{C}$. And then the specimen was unloaded and the low temperature ($T_{tr} - 20^{\circ}\text{C}$) was maintained for 10 min. The specimen was reheated up to $T_{tr} + 20^{\circ}\text{C}$ and maintained for 10 min. Shape recovery and shape fixity are obtained based on the equation (3) and (4).

$$\text{Shape recovery (\%)} = \frac{\varepsilon_m - \varepsilon_r}{\varepsilon_m} \times 100 \quad (3)$$

$$\text{Shape fixability (\%)} = \frac{\varepsilon_f}{\varepsilon_m} \times 100 \quad (4)$$

ε_m = The strain at an 80% compression

ε_f = The strain at $T_{tr} - 20^{\circ}\text{C}$

ε_r = The recovery compression rate at $T_{tr} + 20^{\circ}\text{C}$

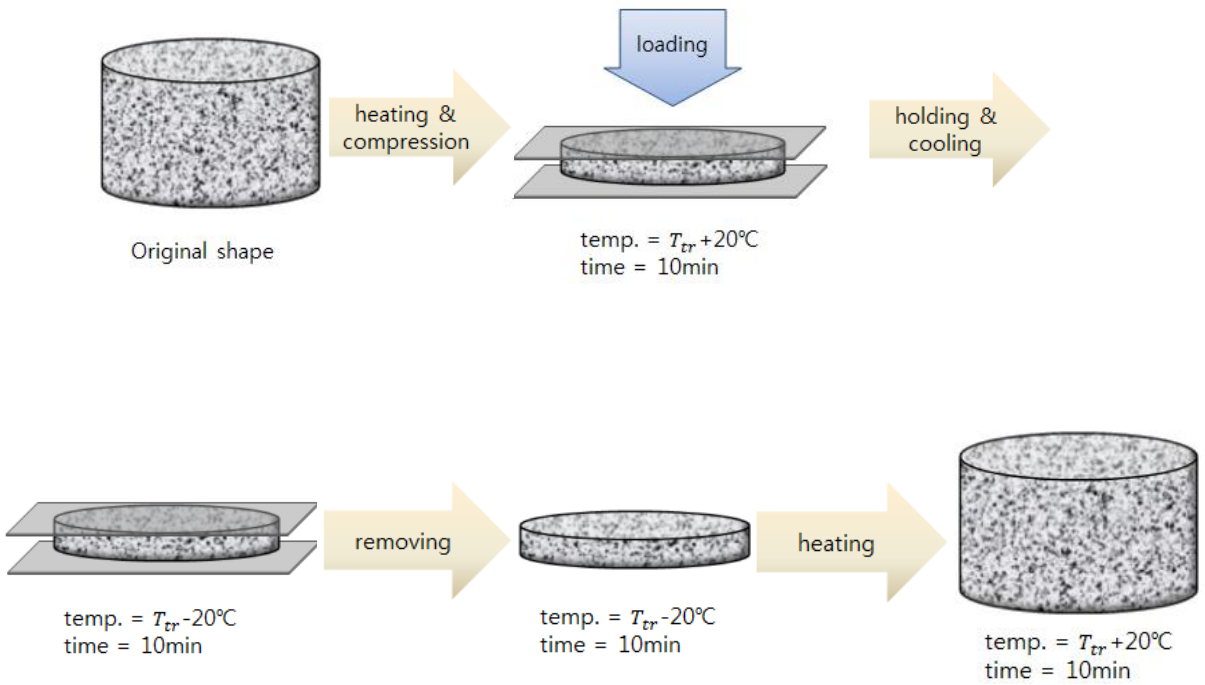


Figure 2.4. Experimental procedure of shape memory effect measurement for SMPU foam.

2.3.7. Mechanical property

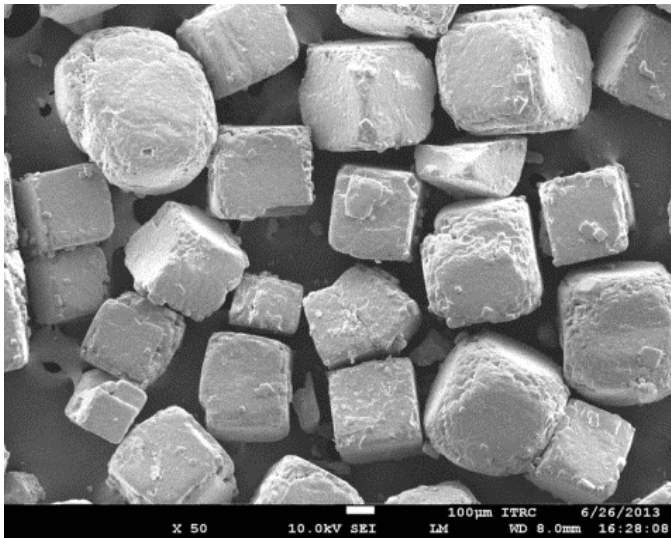
The compressive strength of the SMPU foam was measured at room temperature with a universal tensile machine (UTM) (Instron3365). The specimens were prepared with a size of 35 mm (diameter) x 15 mm (thickness). The crosshead speed of compression was set at 10 mm/min. Compressive stress was measured until the specimens were compressed up to a maximum strain.

III. RESULTS AND DISCUSSION

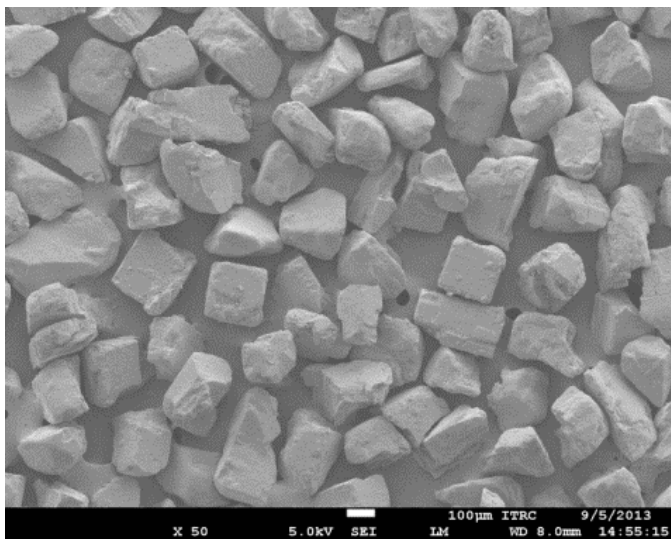
3.1. Morphological properties

3.1.1. Particle sizes of NaCl

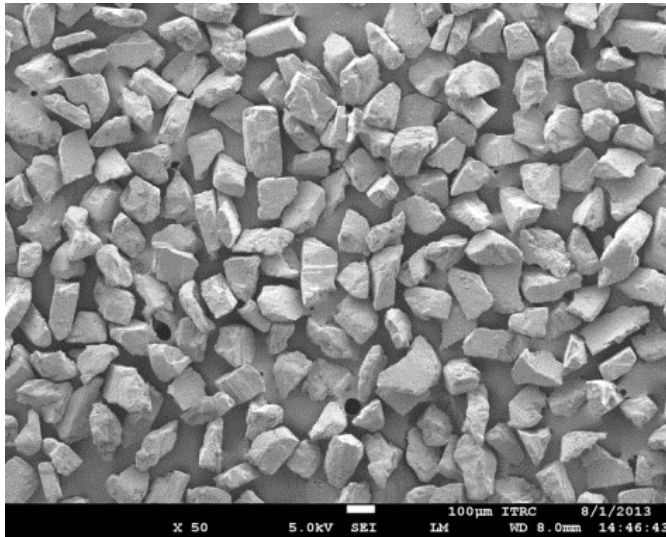
NaCl particles were grinded and filtered with various sizes of sieves in order to fabricate SMPU foam specimens listed in Table 2.1. As shown in the FE-SEM images and particle size analysis data, the average particle diameters of the NaCl particles were 413.8, 242 and 127.5 μm . In the particle size analysis data, diameters of the particles are expressed on the x-axis. The left y-axis of the graph (%passing) presents the accumulative distribution of the particle sizes. The right y-axis of the graph (%channel) denotes the distribution of the particle sizes for each section. Filtered NaCl particles were within the scope of the sieve sizes, respectively.



(a)

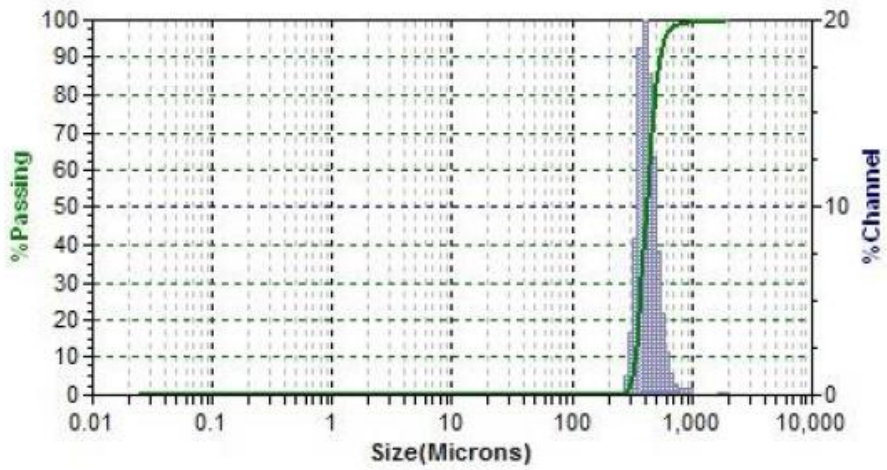


(b)

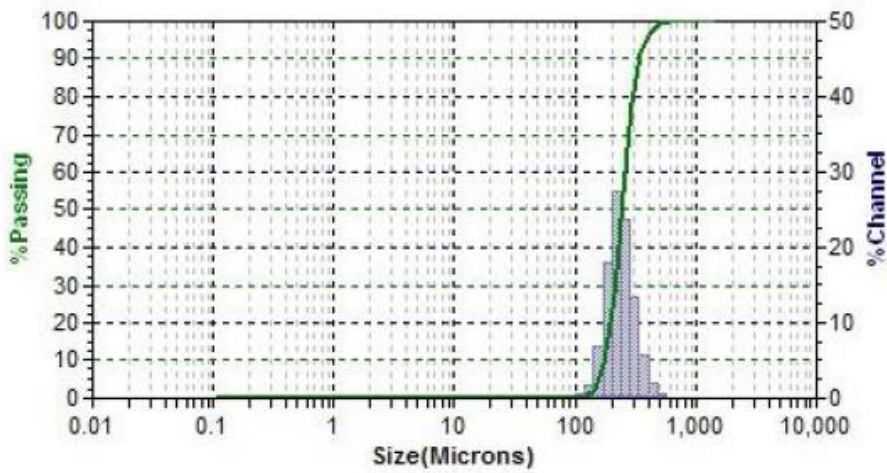


(c)

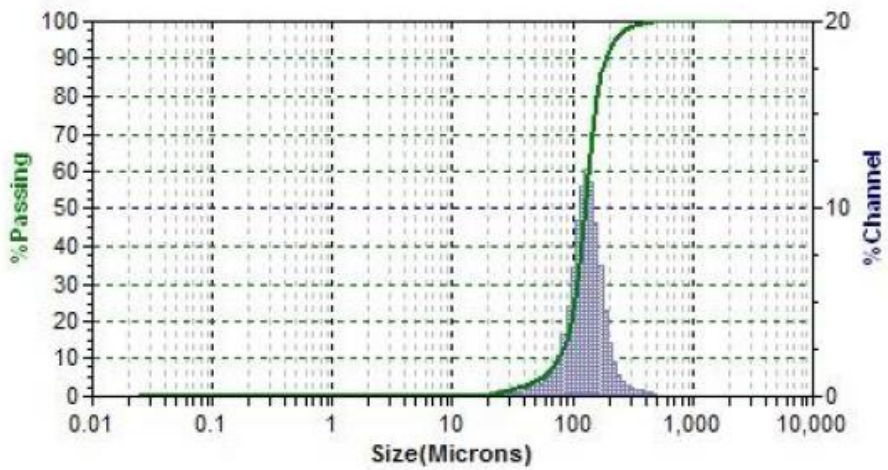
Figure 3.1. SEM images of various size NaCl particles filtered by using different sieves. Average particle sizes of the NaCl were (a) 413.8 (b) 242 (c) 127.5 μm



(a)



(b)



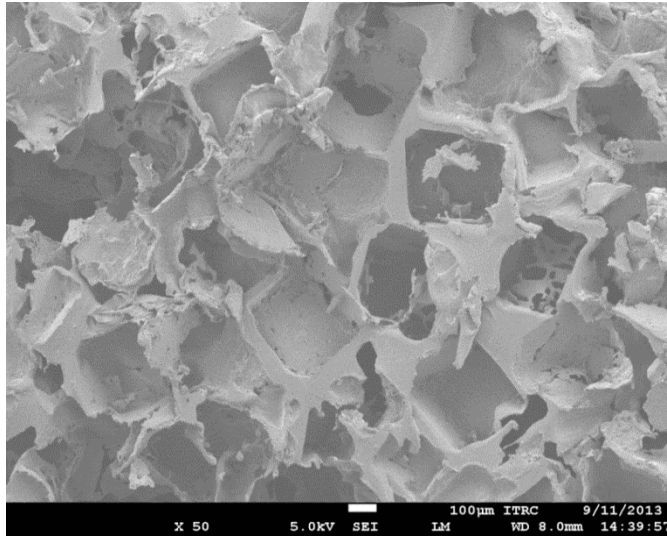
(c)

Figure 3.2. Size distribution of the filtered NaCl particles. Average particle sizes of the NaCl were (a) 413.8 (b) 242 (c) 127.5 μm

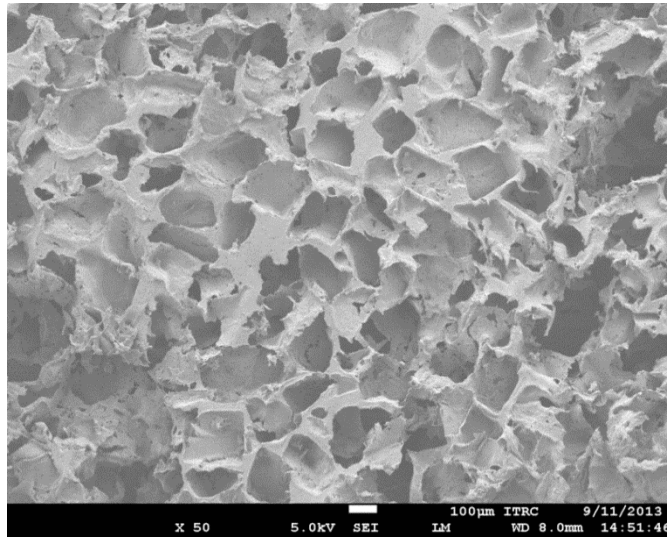
3.1.2. SEM images of SMPU foam

Fig. 3.3 shows the cross sectional images of the SMPU foams which were fabricated by the salt leaching method. The pores were created as the space that the NaCl particles dissolved from SMPU composite, when immersing the SMPU composite in water. The cell size of the SMPU foam tends to be directly related to the size of the NaCl particle in comparison to the SEM images and the particle analysis data of NaCl particles. Hybrid foam has a structure mixed 400 μm sized pores and 100 μm sized pores. Functionally gradient foam composed of 400, 200 and 100 μm sized pores with laminated structure.

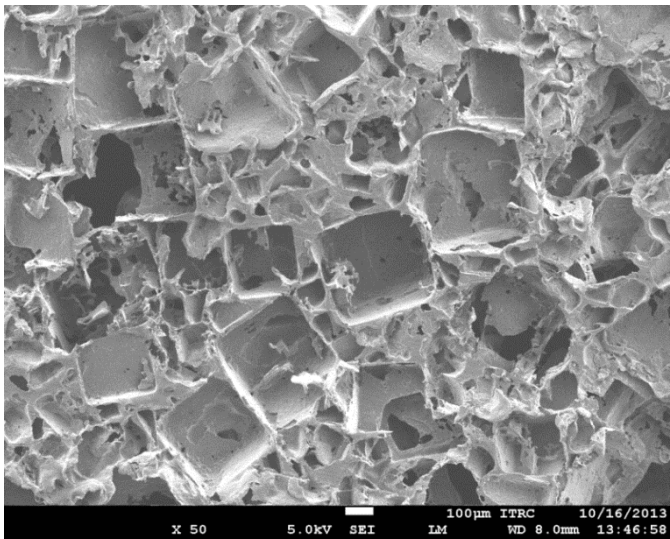
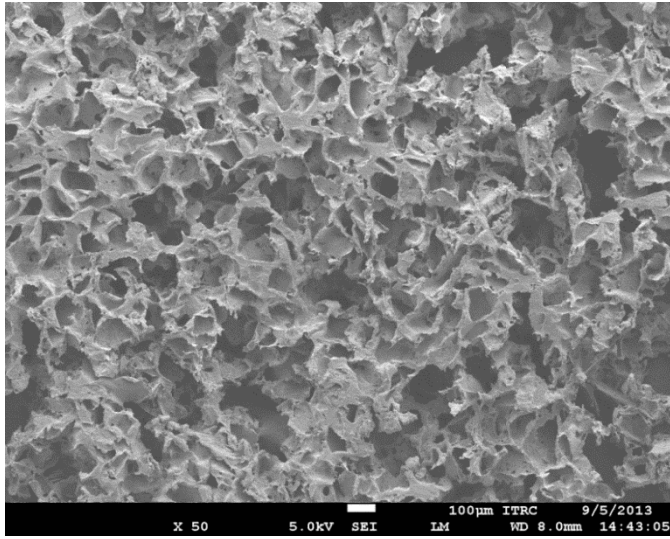
Fig. 3.4 shows the cross sectional images of the original, compressed and recovered SMPU foam. As shown in Fig. 3.4 (b), shape of the pore in the foam becomes flat by compressing SMPU foam and SMPU foam remained as compressed shape at room temperature after it was loaded above T_{tr} . As shown in Fig. 3.4 (c), the thickness of compressed SMPU foam was almost returned to original thickness of SMPU foam when the compressed specimen was heated above T_{tr} .



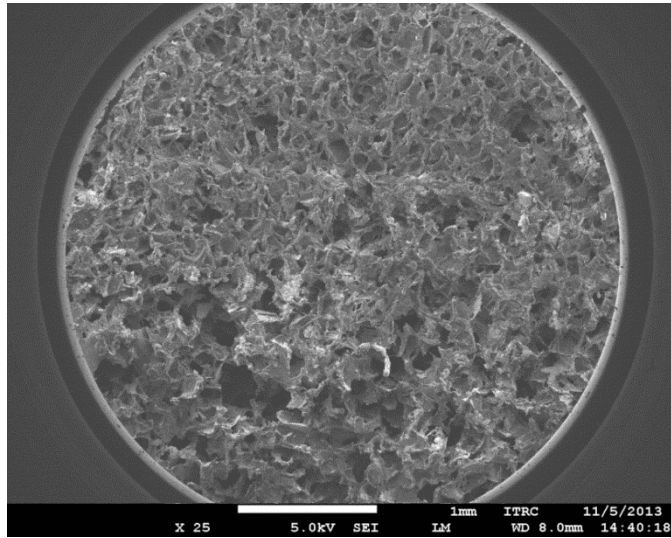
(a)



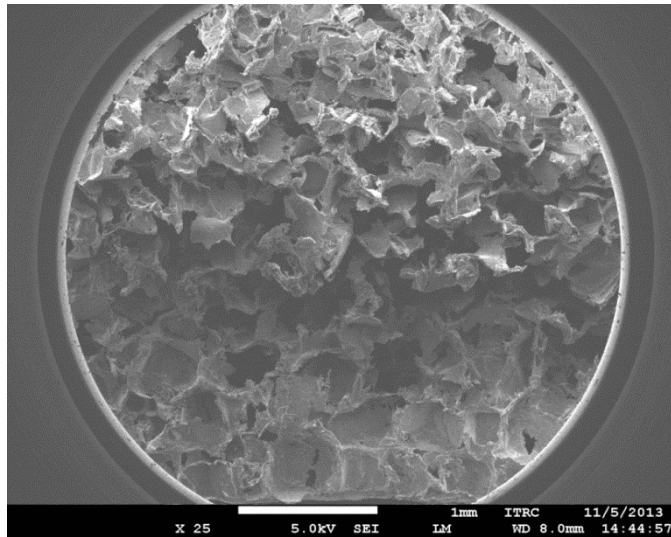
(b)



(d)

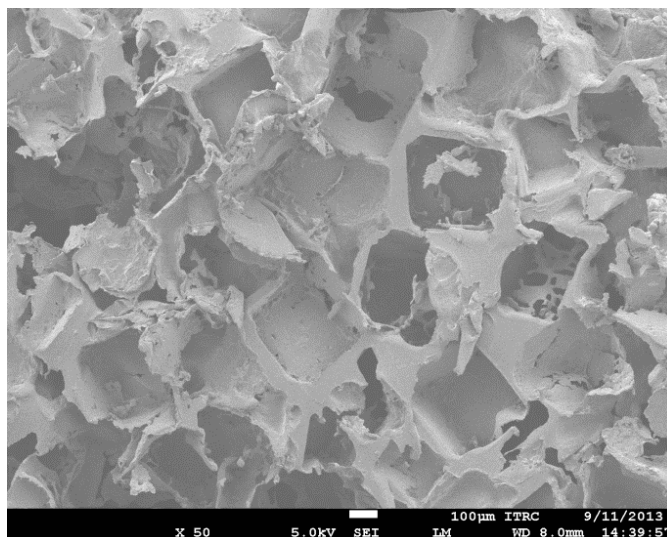


(e)

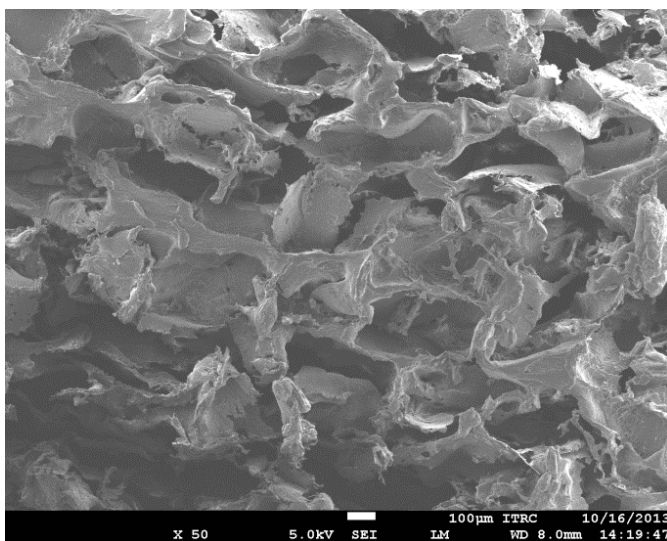


(f)

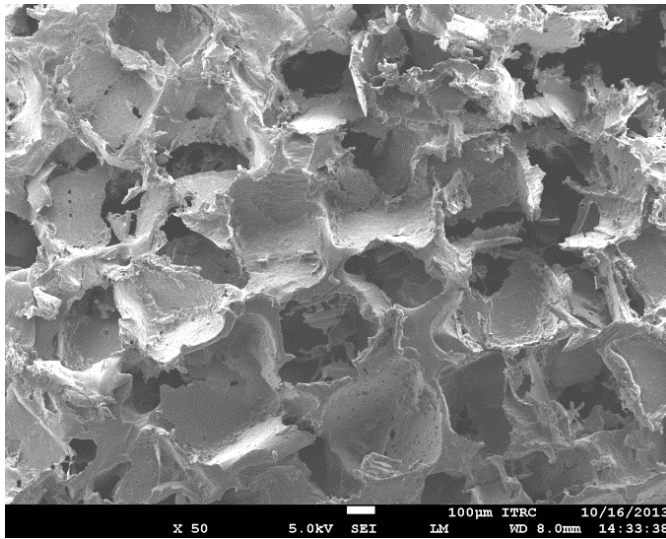
Figure 3.3. SEM images of cross sectional images of SMPU foams: (a) SMPU foam-400 (b) SMPU foam-200 (c) SMPU foam-100 (d) Hybrid foam (e) Functionally gradient foam (f) Functionally gradient foam



(a)



(b)



(c)

Figure 3.4. SEM images of cross sectional images of SMPU foam-400: (a) original shape (b) compressed shape (c) recovered shape

3.1.3. Porosity of SMPU foam

The porosity of the SMPU foam was calculated from the equation (2). The density of the synthesized polyurethane, ρ_p is 1.049 g/cm^3 and ρ_f is the density of the foam material.

The density and porosity of the SMPU foam specimens were listed in Table 3.1. As shown in Table 3.1 and Fig. 3.5, the porosity of the specimens (SMPU foam-400, SMPU foam-200, SMPU foam-100) was in the range from 84 to 85 %. Hybrid foam which manufactured by mixing $400\mu\text{m}$ and $100\mu\text{m}$ sized particles has the highest porosity of 91.7% than other samples because $100 \mu\text{m}$ sized particles were located among $400 \mu\text{m}$ sized particles in the blending process. Functionally gradient foam, which is composed of 400 , 200 and $100 \mu\text{m}$ sized pores with laminated structure, has porosity of 84.7%. It is similar to the porosity of SMPU foam-400, SMPU foam-200 and SMPU foam-100.

Table 3.2 and Fig. 3.6 show the porosity changes with the shape of SMPU foam such as original, compressed and recovered shape. When SMPU foam-400 was compressed, the porosity of the specimen decreased from 85.5 % to 58.7%. After the compressed SMPU foam was recovered its own shape by heating above T_{tr} , the porosity of SMPU foam became 84.6%. It was found that porosity of SMPU foam is recovered through shape recovery of SMPU foam.

Table 3.1. Porosity of SMPU foam specimens.

Samples	Density (g/cm^3)	Porosity (%)
SMPU foam-400	0.152	85.5
SMPU foam-200	0.159	84.8
SMPU foam-100	0.166	84.1
Hybrid foam	0.087	91.7
Functionally gradient foam	0.160	84.7

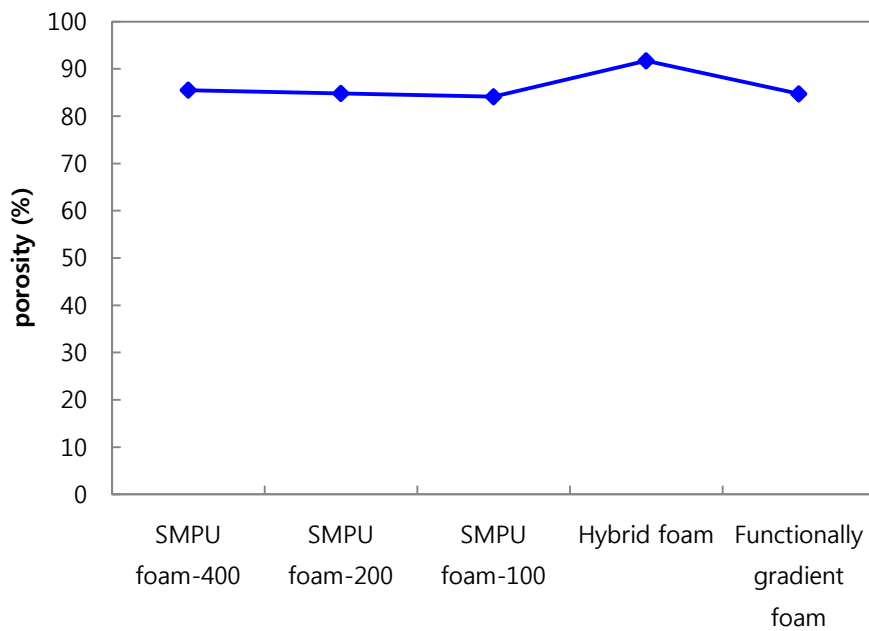


Figure 3.5. Porosity of different SMPU foams having different size of pore (SMPU foam-400, SMPU foam-200, SMPU foam-100) and different structure (hybrid foam, functionally gradient foam).

Table 3.2. Porosity changes with the shape of SMPU foam (original shape, compressed shape, recovered shape).

Shape of sample	Density (g/cm^3)	Porosity (%)
Original shape	0.152	85.5
Compressed shape	0.433	58.7
Recovered shape	0.161	84.6

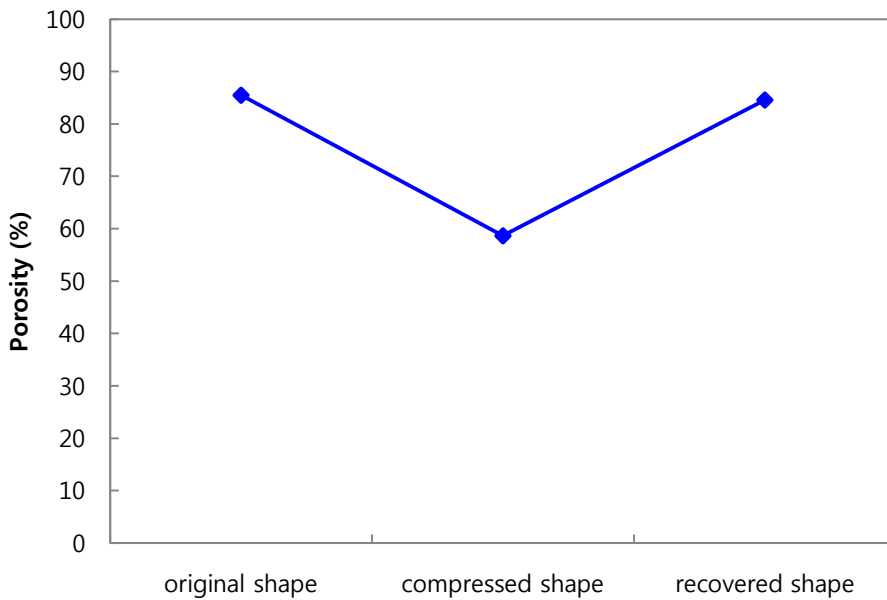


Figure 3.6. Porosity of SMPU foam-400 with the change of the specimen (original shape, compressed shape, recovered shape).

3.2. Thermal properties

3.2.1. DSC results

The transition temperature (T_{tr}) of the SMPU were measured by using DSC. Fig. 3.7 shows the results of the DSC analysis of the SMPU film. The SMPU film showed an endothermic peak by soft segment melting at 53.8°C. The previous researches reported the relation between the transition temperature and molecular structure of SMPU synthesized with PCL as polyol [20, 21]. The transition temperature of SMPU is decided by molecular weight of polyol and mixing ratio of hard segment and soft segment [22]. The transition temperature of the SMPU synthesized in this study is 53.8°C which can remain transformed shape at room temperature and recover original shape above T_{tr} . This SMPU film is qualified for manufacturing the efficient and thermally active insulation material.

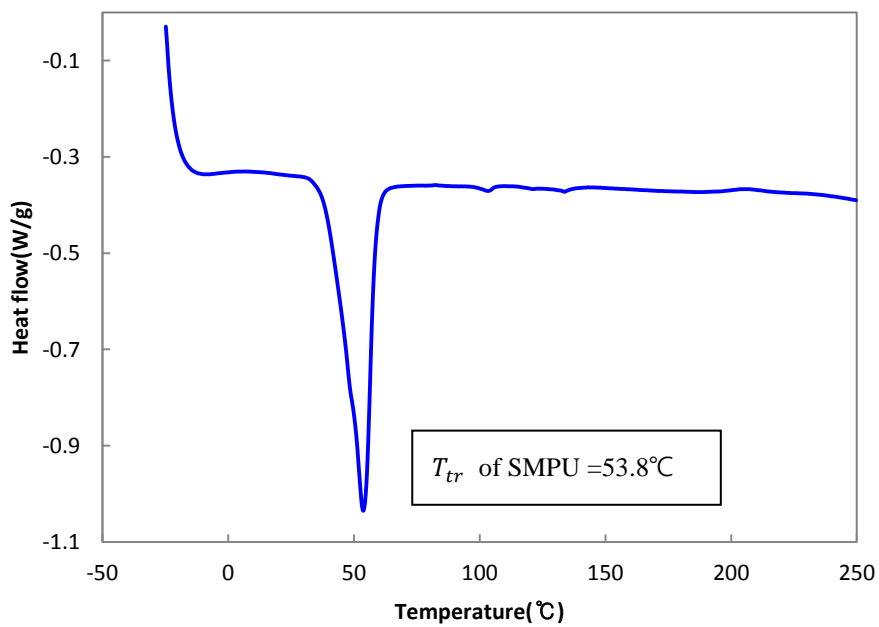


Figure 3.7. The DSC result of the synthesized SMPU which was measured at a heating rate of 10 °C/min.

3.2.2. Thermal conductivity

Table 3.3 and Fig. 3.8 show the thermal conductivity of the specimens. As shown in Fig 3.8., the thermal conductivity of SMPU foam is significantly lower than those of SMPU film. Because SMPU foam is a cellular structure containing gases in a lot of cells.

The thermal conductivity is plotted as a function of the pore size of SMPU foams in Fig. 3.9. The thermal conductivity of the SMPU foam decreases from 0.061 W/m·K to 0.055 W/m·K, when the cell size of foam becomes smaller. Considering the cell size of SMPU foams, the tendency of the thermal conductivity of SMPU foams can be explained by the following reasons. Interfacial thermal resistance between the cells and the solid walls of foam structure is generated in SMPU foam. As reducing the cell size of SMPU foam, the area of a surface in the foam increases. Therefore the increased interfacial thermal resistance disturbs heat transfer of SMPU foam. It is reported that the radiation heat transfer inside the foam is reduced by decreasing the pore size of the foam [23].

The thermal conductivity of hybrid foam is 0.047 W/m·K which is the lowest value in the results. It caused by the increased porosity and surface area in the foam. 100 μm sized pores were generated between 400 μm sized pores therefore the porosity and the surface area increased.

Table 3.3. Thermal conductivity of SMPU foam specimens.

Samples	Thermal conductivity (W/m·K)
SMPU	0.352
SMPU foam-400	0.061
SMPU foam-200	0.059
SMPU foam-100	0.055
Hybrid foam	0.047
Functionally gradient foam	0.059

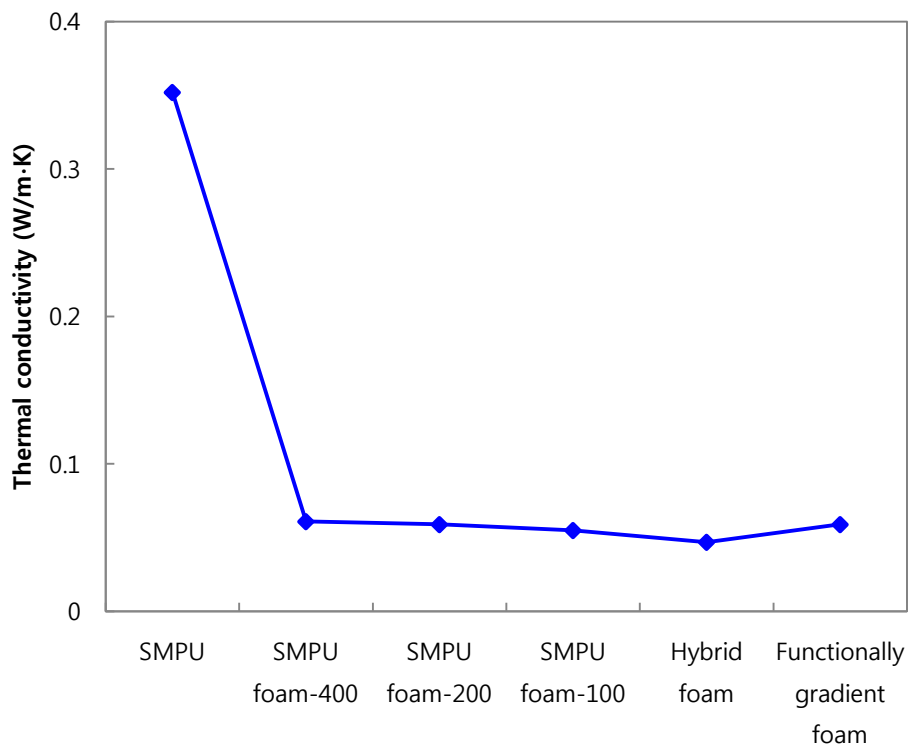


Figure 3.8. Thermal conductivity of the synthesized SMPU and SMPU foams.

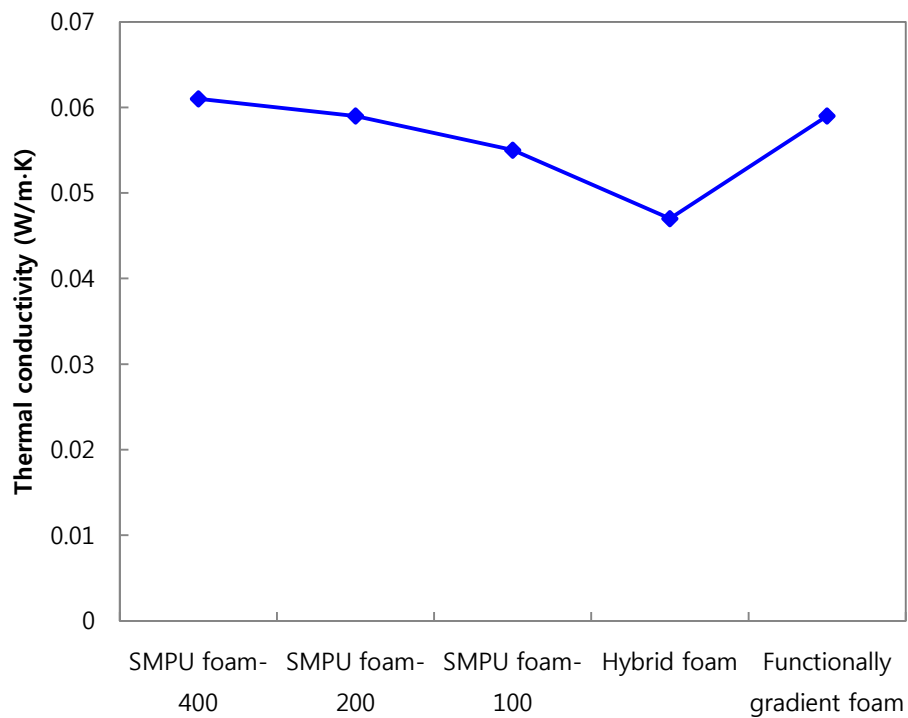


Figure 3.9. Thermal conductivity of the SMPU foams having different pores sizes (SMPU foam-400, SMPU foam-200, SMPU foam-100) and different structure (hybrid foam, functionally gradient foam).

3.2.3. Thermal resistance

Thermal resistance is the temperature difference between two surfaces of a material that induces heat flux through a unit area. Thermal resistance (R) is derived from thermal conductivity (k) and the thickness of materials (L). According to the definition of thermal resistance and the equation of thermal conductivity, thermal resistance can be obtained as,

$$R = \frac{\Delta T}{q} = \frac{L}{k} \quad (5)$$

, where ΔT represents the temperature difference between the hot and the cold temperature, q is heat flux during heat transfer process [24].

Fig. 3.10 and Fig. 3.11 show thermal conductivity and thermal resistance as a function of the shape of SMPU foam such as original specimen, compressed specimen and recovered specimen. The thermal conductivity was increased with compressing the foam from 0.061 to 0.074 W/m·K. After recovering the shape by heating above T_{tr} , the thermal conductivity of the specimen was 0.063 W/m·K. The change of thermal conductivity with the shape of the specimen was caused from the porosity change and according to the morphology transformation. In addition, the thermal resistance of specimens significantly was varied with the thickness of SMPU foam. The thermal resistance of SMPU foam with original shape was $0.25m^2 \cdot K/W$. When SMPU foam was compressed by loading and compressed shape was maintained below T_{tr} , the thermal resistance of

Table 3.4. Thermal resistance of SMPU foam with change of thickness.

Shape of specimen	Thermal conductivity ($W/m \cdot K$)	Thickness (m)	Thermal resistance ($m^2 \cdot K/W$)
Original shape	0.061	0.015	0.25
Compressed shape	0.074	0.003	0.04
Recovered shape	0.063	0.014	0.22

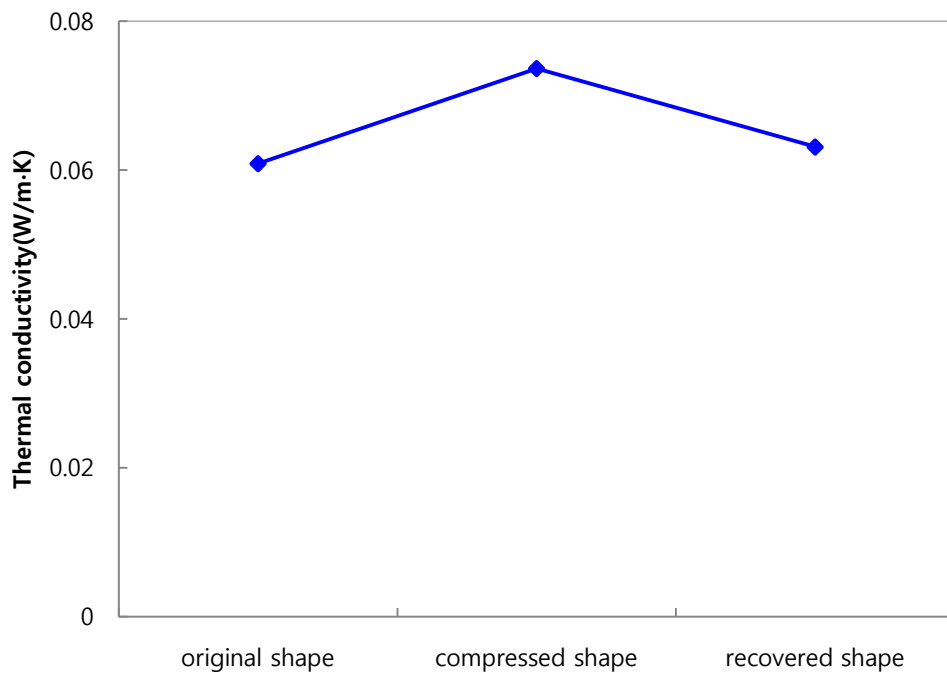


Figure 3.10. Thermal conductivity of SMPU foam with change of thickness of specimen.

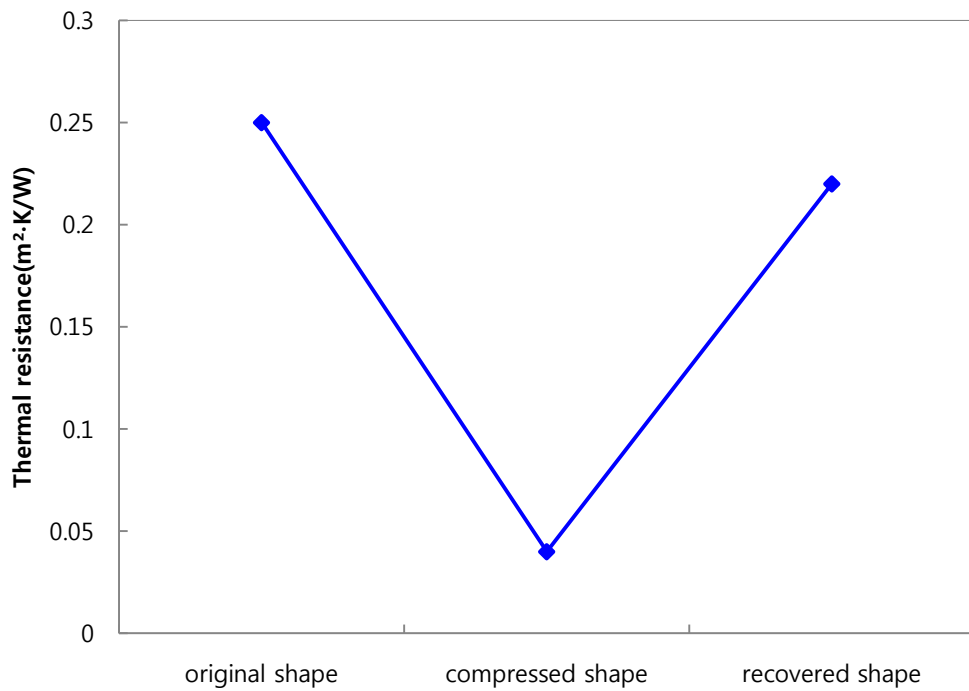


Figure 3.11. Thermal resistance of SMPU foam with change of thickness of specimen.

SMPU foam decreased to $0.04m^2 \cdot K/W$. After the thickness of SMPU foam was recovered, the thermal resistance of the specimen increased to $0.22m^2 \cdot K/W$.

3.3. Shape memory effect of SMPU foam

3.3.1. Shape recovery and fixity

Shape memory effect was measured with the experimental procedure in Fig. 2.4. Shape recovery and shape fixity of SMPU foam are listed in Table 3.5. Shape recovery of the SMPU foam specimens is over 98% and shape fixity is from 97 to 98%. The shape recovery and fixity of the overall specimens are an advanced capability for shape memory effect.

Table 3.5. Shape recovery and fixity of SMPU foams.

	Shape recovery (%)	Shape fixity (%)
SMPU foam-400	98	97
SMPU foam-200	98	97
SMPU foam-100	98	97
Hybrid foam	98	98
Functionally gradient foam	98	97

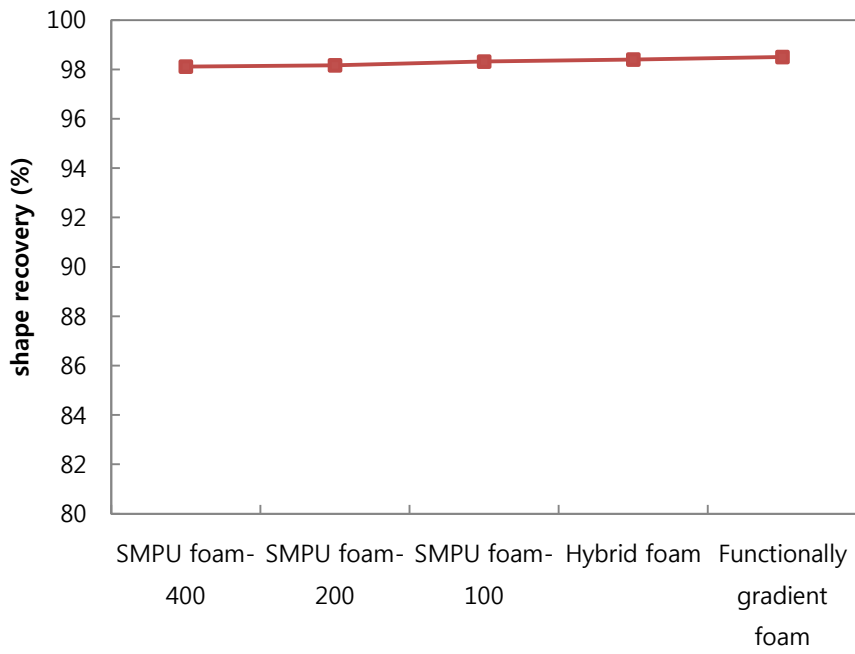


Figure 3.12. Shape recovery of SMPU foam specimens.

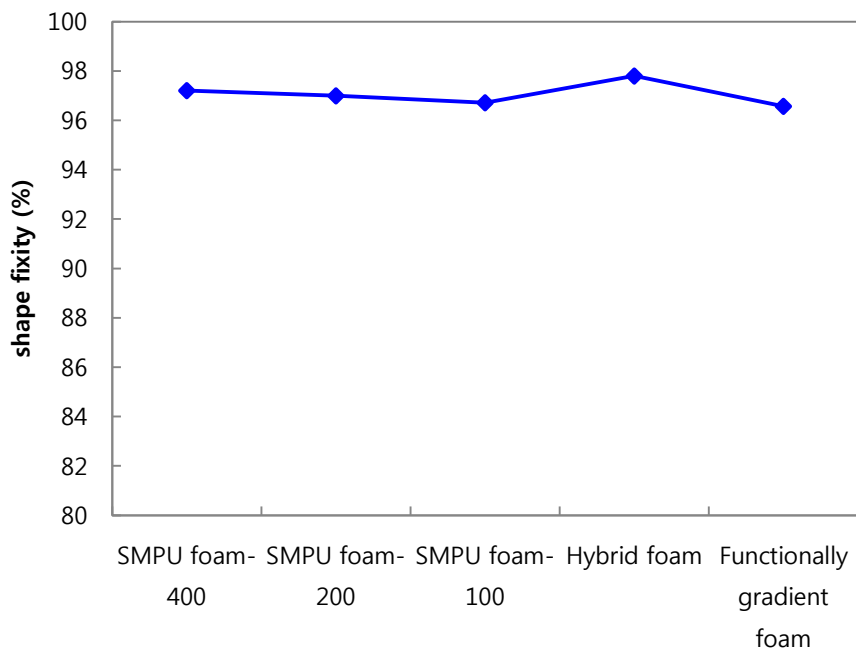


Figure 3.13. Shape fixity of SMPU foam specimens.

3.3.2. Shape memory repeatability

Shape memory repeatability was measured by four times repeating shape recovery test. As shown in Table 3.6 and Fig. 3.14, shape recovery of the specimen reduced from 98% to 92% and shape fixity increased slightly from 97% to 98% after four times cycles. A high level of shape recovery was maintained and shape fixity was improved despite four times repetition of shape recovery test. It confirms that SMPU foam can be used for a long time with repetitive shape deformation.

Table 3.6. Shape recovery and fixity of SMPU foams with increasing of number of cycles.

Number of cycles	1	2	3	4
Shape recovery (%)	98	95	93	92
Shape fixity (%)	97	97	98	98

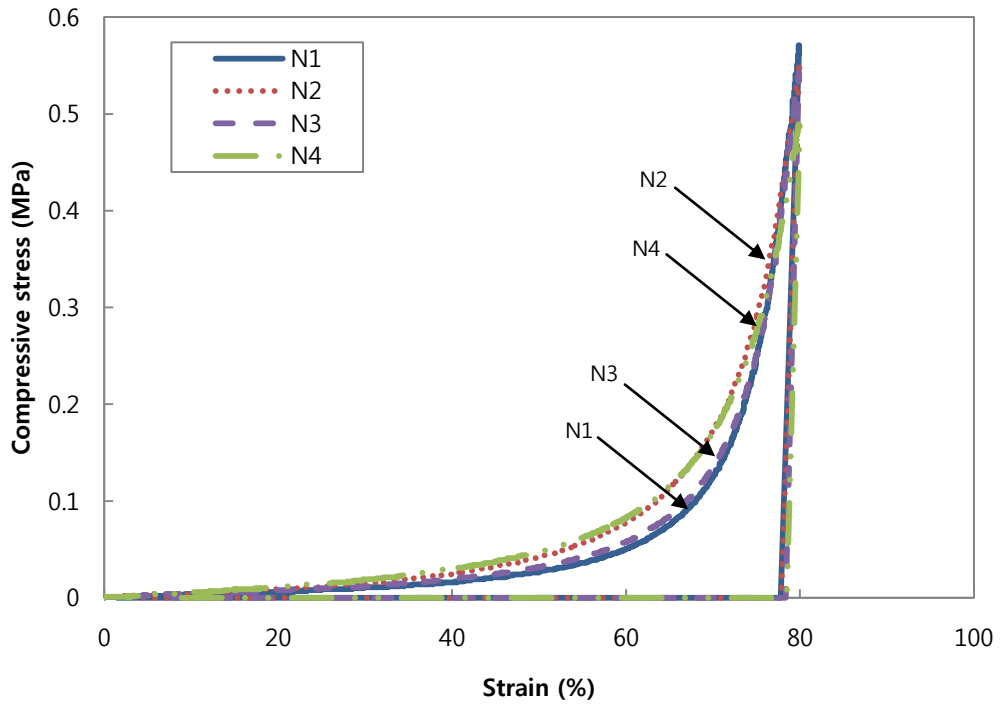


Figure 3.14. The compressive stress-strain curves for the shape memory repeatability of the SMPU foam at a compressive strain rate of 10 mm/min.

3.4. Mechanical properties

Fig. 3.15 shows compressive stress-strain curve of the SMPU foam specimens. As shown in curves of SMPU foam-400, SMPU foam-200 and SMPU foam-100, the compressive strength of SMPU foam was increased with the decrease of pore size. It can be explained by buckling effect. Buckling effect is that the column is suddenly bended, when the compressive load applies to the both ends of the column and the load reaches some stage. The ratio of the length of the column to the cross sectional area is called the slenderness ratio. The long and thin column has high slenderness ratio and buckling phenomenon easily occurs. When pore size increases, the slenderness ratio becomes larger, therefore the compressive strength of the foam decrease by buckling phenomenon [25]. The compressive strength of functionally gradient foam is between those of SMPU foam-200 and SMPU foam-100 by the rule of mixtures.

The compressive strength of hybrid foam is the lowest value. It results from the increased porosity by mixing 400 μm and 100 μm sized particles of NaCl. The buckling phenomenon of the cell walls occurs readily because the walls of the cell in hybrid foam are thinner than those of other samples. The low compressive strength of hybrid foam also can be caused by stress concentration which occurs on the large pores when large pores and small pores are mixed.

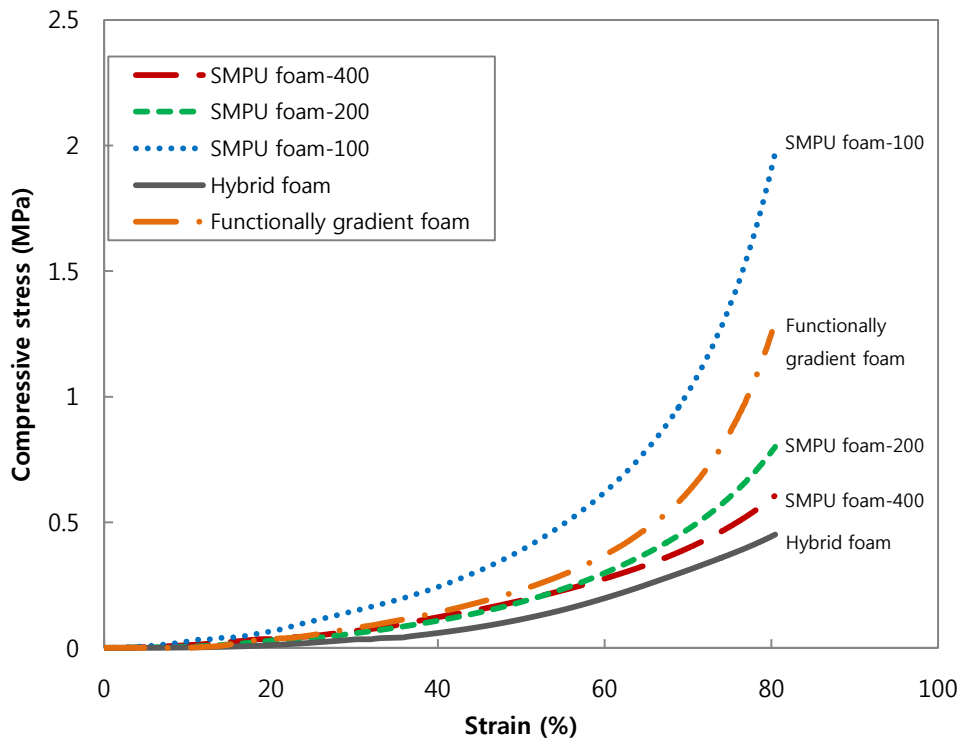


Figure 3.15. The compressive stress-strain curves of the SMPU foam at a compressive strain rate of 10 mm/min.

3.5 Analytic modeling

3.5.1. Heat transfer theory of SMPU foam

Heat transfer mechanisms in foam material are three modes—conduction, convection, and radiation. In general, the convection can be neglected, because the space in each cell is small enough. The contribution of the gas convection to the overall thermal conductivity of the foam is negligible for cell sizes less than 1.5mm. Therefore, the overall thermal conductivity of SMPU foam is determined by conduction and radiation heat transfer.

Conduction heat transfer is explained by Fourier's law,

$$q = -KA \frac{\partial T}{\partial X} \quad (6)$$

where thermal conductivity, K is material constant, q is heat flux, A is the unit area, and $\partial T/\partial X$ is temperature gradient. In order to apply Fourier's law to the foam material, it is necessary to identify the effective thermal conductivity of the foam from the porosity and thermal conductivity of polymer and gas, which are each component of a foam material.

However, the predictive value of the effective thermal conductivity varies with the way to model the structure because foam has complex microstructure. In this study, the effective thermal conductivity is determined with the equation proposed by Glickman [26, 27].

$$K = K_g + \left(\frac{2}{3} - \frac{f_s}{3}\right)(1 - V_g)K_s \quad (7)$$

$$K = K_g + 0.8\left(\frac{2}{3} - \frac{f_s}{3}\right)(1 - V_g)K_s \quad (8)$$

where f_s is the proportion of strut in total polymer, K_g is the conductivity caused by the conduction through the gas, K_s is the conductivity caused by the conduction through the solid, and V_g is the porosity. Equation (7) is the upper value and equation (8) expresses the lowest value. The actual foam material has the effective thermal conductivity between the upper value and the lowest value. These two values are not significantly different, and equation (7) is widely used to predict the thermal conductivity caused by conduction. Equation (7) predicts relatively accurate value of the thermal conductivity caused by conduction in the complex foam material. This equation is mainly utilized to predict the thermal conductivity caused by conduction.

In general, Stefan-Boltzmann equation explains the relation between temperature and heat generated by radiation.

$$q = \varepsilon\sigma AT^4 \quad (9)$$

where σ is Stefan-Boltzmann constant, ε is emissivity, A is radiation area, and T is temperature. Radiation heat transfer of the foam is more complex and more difficult to analyze than conduction heat transfer. Radiation energy can decrease with absorption as well as scattering by strut. Because of these characteristics, it is very difficult to analyze accurately radiation heat transfer

of the foam. It is more appropriate that explain the radiation heat transfer with the experimental data than theoretical analysis. Rosseland's radiation theory is the most reasonable equation by using the experimental data. Radiation heat transfer of the foam can be predicted by substituting extinction coefficient which is resulted from experiment [23, 28].

$$q_r = - \frac{16\sigma T^3}{3K_R} \frac{dT}{dx} \quad (10)$$

where subscript R means Rosseland average which indicate a weighted average about each wavelength, because extinction coefficient varies with wavelength. However, there are various ways to calculate K_R and it is difficult to obtain data experimentally. Therefore, the equation which can explain radiation heat transfer more readily is needed. The following simple equation (11) is suggested when assuming that gas layers and solid layers are parallel to each other and wall is transparent and strut is opaque, and neglecting the decrease of radiation heat by scattering.

$$K_r = \frac{4\sigma\epsilon LT^3}{2-\epsilon} \quad (11)$$

where L is thickness of gas layer which means the cell size. This equation indicates the relation with the thermal conductivity caused by radiation and the cell size. However, the predictive value of the thermal conductivity caused by radiation is more inaccurate than Rosseland's equation. Therefore, correction factor based on experiment is utilized to compensate the defect in this study.

$$K_r = k \frac{4\sigma\epsilon LT^3}{2-\epsilon} \quad (12)$$

where k is a correction factor which is obtained through experiment of this research. Predicted value of the heat transfer by conduction is quite accurate. Therefore, subtracting theoretical value of the thermal conductivity caused by conduction from the experimental value of the overall thermal conductivity is regarded as contribution to the thermal conductivity by radiation. The correction factor, k, is experimental determined to be 3.7 in this study.

3.5.2. Prediction of thermal conductivity of SMPU foam

The overall thermal conductivity of the foam is determined by prediction formulas of conduction and radiation heat transfer, and is expressed by following equation (13).

$$K = K_g + \left(\frac{2}{3} - \frac{f_s}{3}\right) (1 - V_g) K_s + k \frac{4\sigma\epsilon LT^3}{2-\epsilon} \quad (13)$$

Fig. 3.17 shows the thermal conductivity by measurement and the theoretically calculated thermal conductivity according to equation (13). As shown in Fig. 3.17, both predicted and measured thermal conductivity have similar tendency which is reduced as the cell size is decreased. The reduced radiation thermal conductivity by decreased the cell size influenced the overall thermal conductivity.

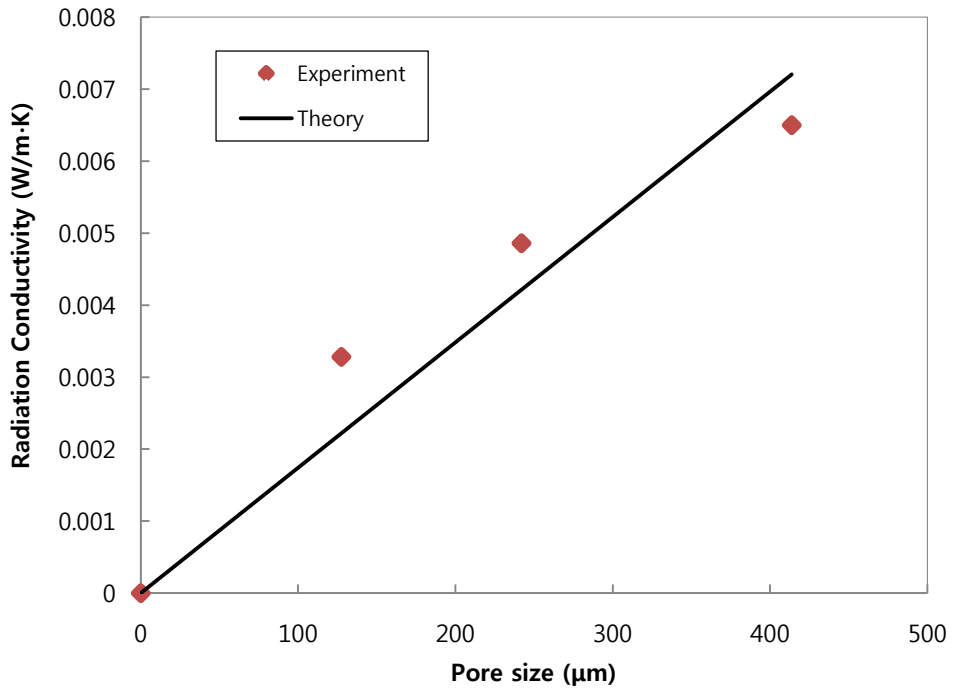


Figure 3.16. Radiation conductivity vs. pore size when density is fixed.

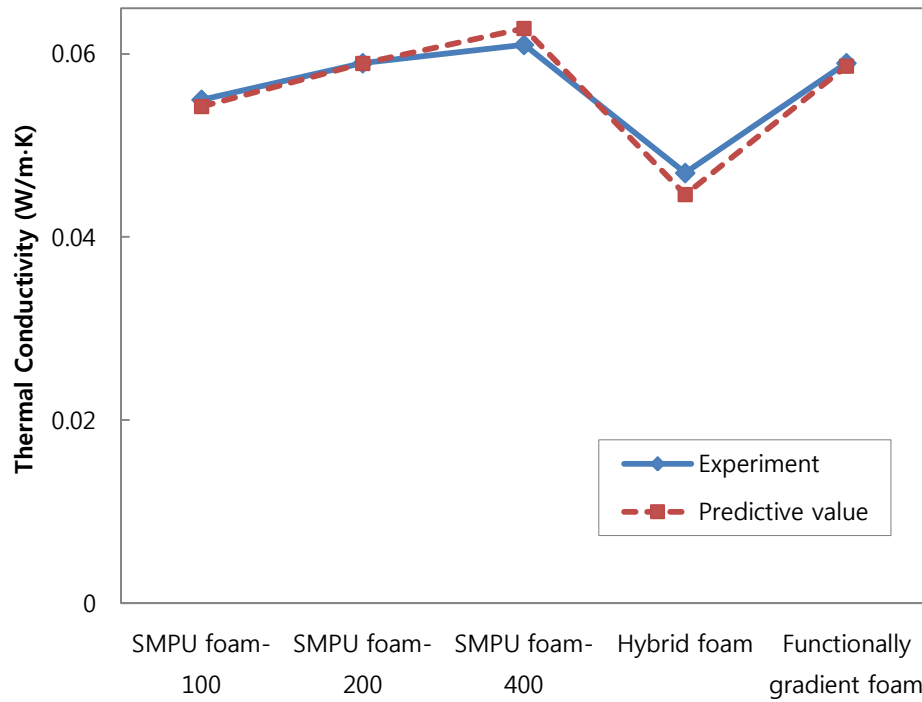


Figure 3.17. Thermal conductivity measured and predicted for different SMPU foam specimens.

V. CONCLUSION

SMPU was synthesized by prepolymerization method to enhance the shape memory effect. Various SMPU foam specimens were prepared by the salt leaching method. Several SMPU foams having different sized pore respectively were produced by using size controlled NaCl particles. Hybrid foam was fabricated by mixing two different sizes of NaCl particles and functionally gradient foam was manufactured by laminating layers of three different sizes of NaCl particles.

Structure of SMPU foam was confirmed by results of FE-SEM. The pores of SMPU foams were obtained by dissolving NaCl particles from SMPU composites in the distilled water. The cell size of the prepared SMPU foam tends to be directly related to the controlled size of NaCl particle. Hybrid foam has pores of 100 μ m among pores of 400 μ m and functionally gradient foam has laminated structure which is composed of pore layers of 400, 200 and 100 μ m. As pore size was decreased, thermal conductivity of the foam was decreased to 0.055W/m·K and compressive strength was increased to 1.97 MPa. It can be seen that SMPU foam with small size pores has excellent insulation properties including the lower thermal conductivity and structure stability. Hybrid foam has the lower thermal conductivity of 0.047 W/m·K and lower compressive strength of 0.45MPa than other SMPU foam specimens.

Thermal conductivity of SMPU foam was decreased from 0.074 to 0.061 W/m·K because the thermal resistance of SMPU foams was increased from 0.04 to 0.25 $m^2 \cdot K/W$ when compressed SMPU foam recovered to original shape.

The SMPU foam was heated above transition temperature after compressing the SMPU foam to investigate the shape memory effect. Shape recovery and shape fixity of the SMPU foam specimens are 98% and 97%, respectively. The result is an excellent capability for shape memory. Shape memory repeatability was obtained by repeating shape recovery test. A high level of shape recovery and shape fixity was represented although the shape recovery test was repeated.

The experimental thermal conductivities of the SMPU foam specimens were compared to the theoretical thermal conductivities of those. The theoretical thermal conductivity of SMPU foam is determined by prediction formulas of conduction and radiation heat transfer. The theoretical thermal conductivities of SMPU foams have similar tendency with the experimental thermal conductivity of those.

SMPU foam has the lower thermal conductivity than other insulation material. Due to the high shape fixity, the compressed SMPU foam occupies a small volume and has wearability at room temperature. It can recover to its original shape to reduce the thermal conductivity of SMPU foam above transition temperature. It will be possible that SMPU foam can

be applied to the intelligent protective clothes used in high temperature environments.

REFERENCES

1. Szycher, M., *Szycher's handbook of polyurethanes*. 1999, Boca Raton: CRC Press.
2. Ferrigno, T.H., *Rigid plastics foams*. 2d ed. 1967, New York,: Reinhold Pub. Corp. xii, 379 p.
3. Koo, M.S., K. Chung, and J.R. Youn, *Reaction injection molding of polyurethane foam for improved thermal insulation*. *Polymer Engineering and Science*, 2001. **41**(7): p. 1177-1186.
4. Thirumal, M., et al., *Effect of foam density on the properties of water blown rigid polyurethane foam*. *Journal of Applied Polymer Science*, 2008. **108**(3): p. 1810-1817.
5. Mikos, A.G., et al., *Laminated 3-Dimensional Biodegradable Foams for Use in Tissue Engineering*. *Biomaterials*, 1993. **14**(5): p. 323-330.
6. Mikos, A.G., et al., *Preparation and Characterization of Poly(L-Lactic Acid) Foams*. *Polymer*, 1994. **35**(5): p. 1068-1077.
7. Behl, M. and A. Lendlein, *Actively moving polymers*. *Soft Matter*, 2007. **3**(1): p. 58-67.
8. Hu, J.L., et al., *Recent advances in shape-memory polymers: Structure, mechanism, functionality, modeling and applications*. *Progress in Polymer Science*, 2012. **37**(12): p. 1720-1763.
9. Lendlein, A. and S. Kelch, *Shape-memory polymers*. *Angewandte Chemie-International Edition*, 2002. **41**(12): p. 2034-2057.
10. Jeon, H.G., P.T. Mather, and T.S. Haddad, *Shape memory and nanostructure in poly(norbornyl-POSS) copolymers*. *Polymer International*, 2000. **49**(5): p. 453-457.
11. Kim, B.K., S.Y. Lee, and M. Xu, *Polyurethanes having shape memory effects*. *Polymer*, 1996. **37**(26): p. 5781-5793.
12. Skochdopole, R., *The thermal conductivity of foamed plastics*.

- 1962.
13. J. Goto, K.S., S. Mashiko, Y. Kataoka, Y. Kambara, I. Ohki, *Development of All Water-Blown Polyurethane Rigid Foam for Housing Insulation.*, in *Polyurethane World Congress 1997: Amsterdam*. p. 17.
 14. Jang, M.S. and J.R. Youn, *Prediction of Thermal Conductivity for Polyurethane Foam with Structural Change*, in *Dept. of Fiber and Polymer Science*. 1998, Seoul National University.
 15. Chung, S.E. and C.H. Park, *The Thermoresponsive Shape Memory Characteristics of Polyurethane Foam*. *Journal of Applied Polymer Science*, 2010. **117**(4): p. 2265-2271.
 16. 박정희, 정승은, and 유웅렬, *형상기억 폴리우레탄 품의 제조 방법 및 이로부터 제조된 형상기억 폴리우레탄 품*. 2012: Korea.
 17. Liao, C.J., et al., *Fabrication of porous biodegradable polymer scaffolds using a solvent merging/particulate leaching method*. *Journal of Biomedical Materials Research*, 2002. **59**(4): p. 676-681.
 18. Nangrejo, M.R. and M.J. Edirisinghe, *Porosity and strength of silicon carbide foams prepared using preceramic polymers*. *Journal of Porous Materials*, 2002. **9**(2): p. 131-140.
 19. Reignier, J. and M.A. Huneault, *Preparation of interconnected poly(epsilon-caprolactone) porous scaffolds by a combination of polymer and salt particulate leaching*. *Polymer*, 2006. **47**(13): p. 4703-4717.
 20. Li, F.K., et al., *Crystallinity and morphology of segmented polyurethanes with different soft-segment length*. *Journal of Applied Polymer Science*, 1996. **62**(4): p. 631-638.
 21. Li, F.K., et al., *Studies on thermally stimulated shape memory effect of segmented polyurethanes*. *Journal of Applied Polymer Science*, 1997. **64**(8): p. 1511-1516.
 22. Ratna, D. and J. Karger-Kocsis, *Recent advances in shape memory polymers and composites: a review*. *Journal of*

- Materials Science, 2008. **43**(1): p. 254-269.
23. Glicksman, L., M. Schuetz, and M. Sinofsky, *Radiation Heat-Transfer in Foam Insulation*. International Journal of Heat and Mass Transfer, 1987. **30**(1): p. 187-197.
 24. Chen, Q. and J.X. Ren, *Generalized thermal resistance for convective heat transfer and its relation to entransy dissipation*. Chinese Science Bulletin, 2008. **53**(23): p. 3753-3761.
 25. Rusch, K.C., *Load-Compression Behavior of Flexible Foams*. Journal of Applied Polymer Science, 1969. **13**(11): p. 2297-&.
 26. Glicksman, L. and M. Torpey. *The influence of cell size and foam density on the thermal conductivity of foam insulation*. in *Polyurethanes World Congress, Aachen, Germany*. 1987.
 27. Kuhn, J., et al., *Thermal Transport in Polystyrene and Polyurethane Foam Insulations*. International Journal of Heat and Mass Transfer, 1992. **35**(7): p. 1795-1801.
 28. Hottel, H. and A. Sarofim, *Radiative heat transfer*. M cGraw—Hill. New York, 1967.

초 록

폼 물질은 낮은 열전도도 뿐만 아니라 형태 안정성을 지니고 있기 때문에 단열재료로 널리 사용되고 있다. 본 연구에서는 더욱 효과적이고 능동적인 단열재료를 개발하기 위하여 형상기억 폴리우레탄 폼을 제조하였으며, 열전도도를 측정하였다. 또한 열전도도와 폼의 미세구조의 관계에 대해 연구하여 효율적인 단열성능을 지니는 구조를 제안하였으며, 열전도도의 이론적인 예측값을 구하여 측정값과 비교 분석하였다.

형상기억 폴리우레탄은 prepolymerization 방법으로 합성되었다. 합성된 형상기억 폴리우레탄의 전이온도를 파악하기 위하여 DSC 분석을 하였다. 형상기억 폴리우레탄 폼은 salt leaching 방법으로 제조되었으며, NaCl 입자 크기를 조절하여 형상기억 폴리우레탄 폼의 기공 크기를 조절하였다. 또한 salt leaching 의 장점을 이용하여 서로 다른 크기의 기공이 섞여있는 Hybrid foam 과 다른 크기의 기공들이 각각 층을 이루고 있는 Functionally gradient foam 을 제조하였다. 제조한 형상기억 폴리우레탄 폼의 열전도도, 기계적 강도, 형상회복력 및 열저항 등 물성 측정과 분석을 통하여 단열성능과 형태안정성을 향상시킬 수 있는 단열재료 모델을 제안하였다.

형상기억 폴리우레탄 폼은 상온에서 압축된 형태를 유지하기 때문에 공간확보와 wearability 에 유리하고, 전이온도 이상의 환경에서는 원래 형상을 회복하여 열저항이 증가한다는 장점을 지니고 있다. 따라서 형상기억 폴리우레탄 폼은 능동적인 지능형 단열재료로 응용이 가능할 것으로 기대된다.

주요어 : 형상기억 폴리우레탄, 폼 물질, 열전도도, 단열재료

학번 : 2012-20588